MALARIA

A long-duration dihydroorotate dehydrogenase inhibitor (DSM265) for prevention and treatment of malaria

Margaret A. Phillips,[1]* Julie Lotharius,[2] Kennan Marsh,[3] John White,[4] Anthony Dayan,[2] Karen L. White,[5] Jacqueline W. Njoroge,[1] Farah El Mazouni,[1] Yanbin Lao,[3] Sreekanth Kokkonda,[4] Diana R. Tomchick,[6] Xiaoyi Deng,[1] Trevor Laird,[2] Sangeeta N. Bhatia,[7] Sandra March,[7] Caroline L. Ng,[8] David A. Fidock,[8,9] Sergio Wittlin,[10,11] Maria Lafuente-Monasterio,[12] Francisco Javier Gamo Benito,[12] Laura Maria Sanz Alonso,[12] Maria Santos Martinez,[12] Maria Belen Jimenez-Diaz,[12] Santiago Ferrer Bazaga,[12] Iñigo Angulo-Barturen,[12] John N. Haselden,[12] James Louttit,[13] Yi Cui,[13] Arun Sridhar,[13] Anna-Marie Zeeman,[14] Clemens Kocken,[14] Robert Sauerwein,[15] Koen Dechering,[15] Vicky M. Avery,[16] Sandra Duffy,[16] Michael Delves,[17] Robert Sinden,[17] Andrea Ruecker,[17] Kristina S. Wickham,[18] Rosemary Rochford,[18] Janet Gahagen,[19] Lalitha Iyer,[19] Ed Riccio,[19] Jon Mirsalis,[19] Ian Bathhurst,[2] Thomas Rueckle,[2] Xavier Ding,[2] Brice Campo,[2] Didier Leroy,[2] M. John Rogers,[20] Pradipsinh K. Rathod,[4] Jeremy N. Burrows,[2] Susan A. Charman[5]*

Malaria is one of the most significant causes of childhood mortality, but disease control efforts are threatened by resistance of the *Plasmodium* parasite to current therapies. Continued progress in combating malaria requires development of new, easy to administer drug combinations with broad-ranging activity against all manifestations of the disease. DSM265, a triazolopyrimidine-based inhibitor of the pyrimidine biosynthetic enzyme dihydroorotate dehydrogenase (DHODH), is the first DHODH inhibitor to reach clinical development for treatment of malaria. We describe studies profiling the biological activity, pharmacological and pharmacokinetic properties, and safety of DSM265, which supported its advancement to human trials. DSM265 is highly selective toward DHODH of the malaria parasite *Plasmodium*, efficacious against both blood and liver stages of *P. falciparum*, and active against drug-resistant parasite isolates. Favorable pharmacokinetic properties of DSM265 are predicted to provide therapeutic concentrations for more than 8 days after a single oral dose in the range of 200 to 400 mg. DSM265 was well tolerated in repeat-dose and cardiovascular safety studies in mice and dogs, was not mutagenic, and was inactive against panels of human enzymes/receptors. The excellent safety profile, blood- and liver-stage activity, and predicted long half-life in humans position DSM265 as a new potential drug combination partner for either single-dose treatment or once-weekly chemoprevention. DSM265 has advantages over current treatment options that are dosed daily or are inactive against the parasite liver stage.

INTRODUCTION

Malaria remains a significant global health challenge and, despite effective drugs and insect control programs, still kills up to 580,000 people each year, the majority being children under 5 years old living in sub-Saharan Africa (*1*–*3*). No other parasitic infection has had such a broad-ranging effect on human health. Its persistence has influenced the evolution of the human genome as highlighted by genetic polymorphisms that have arisen by conferring protection against severe malaria (*1*). Today, 3 billion people are at risk of malaria in 97 countries, leading to 200 million cases annually caused primarily by *Plasmodium falciparum* and *Plasmodium vivax*. Pregnant women and nonimmune naïve hosts are also particularly susceptible to severe disease, which is associated with complications such as severe anemia and/or sequestration of parasitized red blood cells (RBCs) into key organs, including brain (*1*). Lack of a fully protective vaccine, the constant threat of drug and insecticide resistance, and poverty all contribute to the difficult task of malaria control and elimination. In areas of intense malaria transmission, children are highly susceptible but adults develop protective immunity and, while harboring parasites, are largely asymptomatic. This reservoir of asymptomatic carriers contributes to transmission and further complicates the goal of malaria eradication (*4*).

Drug therapy provides the most effective option for treatment and prevention of malaria, and a broad portfolio of clinically effective drugs has been developed and used throughout the modern history of the disease (*1*, *5*). The propensity of the parasite to develop resistance to many of these agents (for example, chloroquine and pyrimethamine)

[1]Department of Pharmacology, University of Texas Southwestern Medical Center at Dallas, 6001 Forest Park Boulevard, Dallas, TX 75390–9041, USA. [2]Medicines for Malaria Venture, 1215 Geneva, Switzerland. [3]Abbvie, 1 North Waukegan Road, North Chicago, IL 60064–6104, USA. [4]Departments of Chemistry and Global Health, University of Washington, Seattle, WA 98195, USA. [5]Centre for Drug Candidate Optimisation, Monash Institute of Pharmaceutical Sciences, Monash University, Parkville, Victoria 3052, Australia. [6]Department of Biophysics, University of Texas Southwestern Medical Center at Dallas, Dallas, TX 75390–9041, USA. [7]Health Sciences and Technology/Institute for Medical Engineering and Science, Massachusetts Institute of Technology, Cambridge, MA 02139, USA. [8]Department of Microbiology and Immunology, Columbia University Medical Center, New York, NY 10032, USA. [9]Division of Infectious Diseases, Department of Medicine, Columbia University Medical Center, New York, NY 10032, USA. [10]Swiss Tropical and Public Health Institute, Socinstrasse 57, 4002 Basel, Switzerland. [11]University of Basel, 4003 Basel, Switzerland. [12]GlaxoSmithKline (GSK), Tres Cantos Medicines Development Campus, Severo Ochoa, Madrid 28760, Spain. [13]GSK, Park Road, Ware, Hertfordshire SG12 0DP, UK. [14]Biomedical Primate Research Centre, P.O. Box 3306, 2280 GH Rijswijk, Netherlands. [15]TropIQ Health Sciences, 6525 GA Nijmegen, Netherlands. [16]Discovery Biology, Eskitis Institute for Drug Discovery, Griffith University, Nathan, Queensland 4111, Australia. [17]Imperial College of Science Technology and Medicine, London SW7 2AY, UK. [18]State University of New York Upstate Medical University, Syracuse, NY 13210, USA. [19]SRI International, Menlo Park, CA 94025, USA. [20]National Institutes for Allergy and Infectious Diseases, 6610 Rockledge Drive, Bethesda, MD 20892, USA.
*Corresponding author. E-mail: margaret.phillips@utsouthwestern.edu (M.A.P.); susan.charman@monash.edu (S.A.C.)

has hindered treatment and control. There is only a single drug for treatment of *P. vivax* latent liver forms (primaquine), and it is contraindicated in glucose-6-phosphate dehydrogenase (G6PD)–deficient patients (*6*), whereas chemopreventive medicines either have concerning side effects (mefloquine) or are expensive and require daily dosing (atovaquone-proguanil) (*1*, *5*). The effectiveness of the artemisinin-based combination therapies for malaria treatment, combined with widespread use of insecticide-treated bed nets, has been credited with reduction in malaria deaths over the past decade. However, resistance to the artemisinins, manifested as delayed parasite clearance and linked to K13-propeller protein polymorphisms, has emerged in South East Asia and is threatening to derail malaria control efforts (*7*).

Over the past decade, a robust effort in antimalarial drug discovery has generated a broad portfolio of new drug candidates (*5*, *8*, *9*). To reduce the potential for emergence of resistance, new treatments are being developed as combination therapies (*10*). Candidate molecules with a broad spectrum of activities including treatment of the blood-stage infection, chemoprevention via activity on liver stages, and transmission-blocking activity are required to contribute to the eradication agenda (*11*). Also, key to this effort is improving patient compliance; thus, compounds with pharmacokinetic properties supporting use in single-dose combination treatments or once-weekly chemoprevention are being prioritized for development.

Extensive and rapid replication of parasite DNA is required to propagate *Plasmodium* species in both liver and blood stages of infection (*1*). As a consequence, several clinically used antimalarial drugs target pyrimidine nucleotide biosynthesis, including the dihydrofolate reductase inhibitors pyrimethamine and P218 (*9*), and the cytochrome bc_1 inhibitor atovaquone (*12*). *Plasmodium* species lack pyrimidine salvage enzymes and, unlike humans, rely entirely on the de novo pathway to acquire pyrimidines for DNA and RNA synthesis. A key step in this pathway is catalyzed by dihydroorotate dehydrogenase (DHODH) (*13*). We previously identified *P. falciparum* DHODH (*Pf* DHODH) inhibitors from the triazolopyrimidine structural class with potent antimalarial activity (*13*). The series was optimized using an x-ray structure–guided medicinal chemistry program, leading to the identification of potent DHODH inhibitors with good pharmacokinetic properties and in vivo efficacy in the *P. falciparum* severe combined immunodeficient (SCID) mouse model (*14*, *15*). Herein, we describe the preclinical development of one of these analogs, DSM265 (Fig. 1A), the first DHODH inhibitor to advance to human clinical trials for the treatment of malaria.

RESULTS

X-ray structure of DSM265 bound to *Pf*DHODH

DHODH is an FMN-dependent mitochondrial enzyme that catalyzes oxidation of dihydroorotate (DHO) to orotic acid in a two-step reaction that requires coenzyme Q (CoQ) for reoxidation of FMN (*13*). The crystal structure of DSM265 bound to *Pf*DHODH was solved for two different crystal forms to 2.25 Å (form I) and 2.8 Å (form II) resolution, respectively (table S1 and fig. S1). The inhibitor binding site is displayed for crystal form II because it had a more uniform DSM265-ligand density. The higher-resolution structure determination of crystal form I allowed better quality refinement of the form II protein structure coordinates. DHODH is composed of a core β/α barrel with an N-terminal α helix that interacts with the mitochondrial membrane, allowing binding of CoQ. The DSM265 inhibitor binding pocket sits between FMN and the N-terminal α helix, and is also thought to be the binding site for CoQ. This pocket is primarily hydrophobic, and only two hydrogen bonds are formed between DSM265 and the protein via Arg^{265} and His^{185} (Fig. 1B). The amino acid composition of the binding site is highly variable between the *Plasmodium* and human enzymes (Fig. 1B and fig. S2), and this property is thought to underlie the strong selectivity for the parasite enzyme over human DHODH (*13*).

Activity and species selectivity of DSM265 and analogs against DHODH

DSM265 is a potent inhibitor of the *Plasmodium* enzymes *Pf* DHODH and *P. vivax* DHODH (*Pv*DHODH) with excellent selectivity versus human DHODH (*14*). To assess species selectivity toward other mammalian or parasite enzymes, we evaluated DSM265 inhibitory activity toward DHODHs from species that would potentially be used in either toxicity or efficacy testing (Table 1). Given that the main impurity (DSM430) and the primary in vivo metabolite (DSM450) of DSM265 (Fig. 1A) (described below) would both be present after in vivo dosing, both compounds were also profiled for species selectivity. DSM265 inhibitory activity versus mammalian DHODHs showed significant differences. Like the human enzyme, rabbit, pig, and monkey DHODHs were not significantly inhibited [50% inhibitor concentration (IC_{50}) > 41 μg/ml]. In contrast, dog DHODH (IC_{50} = 10 μg/ml), and to a greater extent the mouse and rat enzymes (IC50 ~ 1 μg/ml for each), were sensitive to DSM265 (Table 1 and Fig. 2A). Comparison of the amino acid sequence in the inhibitor binding site shows that the rodent DHODH binding sites have diverged from human DHODH at four positions (M111L, F62V in rat and mouse, T360I in rat, and T63I in mouse), whereas dog DHODH differs at only one (F62V) (fig. S2). The remaining mammalian enzymes

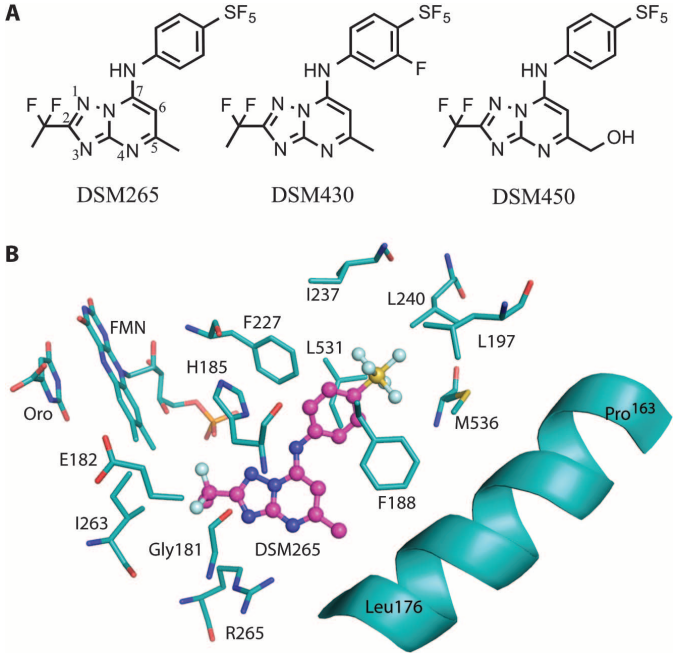

Fig. 1. Chemical and protein-bound inhibitor structures. (**A**) Chemical structures of DSM265 (415 daltons), DSM430 (430 daltons), and DSM450 (431 daltons). (**B**) X-ray structure of the inhibitor binding site of *Pf* DHODH bound to DSM265 [Protein Data Bank (PDB) 5BOO]. DSM265 (pink); protein, orotate (Oro), and flavin mononucleotide (FMN) (carbons in teal); oxygen (red); nitrogen (blue); sulfur (yellow); phosphate (orange); and fluorine (light blue).

Table 1. Comparative kinetic analysis of DSM265 and derivatives on *P. falciparum* and mammalian DHODH. Data represent mean of three technical replicates with 95% confidence intervals for the fit shown in parentheses. Primary data are provided in table S19. ND, not determined.

Compound	DSM265	DSM430	DSM450
DHODH		**IC_{50} (μg/ml)**	
P. falciparum	0.010 (0.0080–0.013)	0.010 (0.0079–0.014)	0.032 (0.026–0.040)
P. vivax	0.020 (0.017–0.024)	ND	0.11 (0.081–0.15)
P. cynomolgi	0.0050 (0.0042–0.0058)	ND	ND
Human	~41	3.7 (2.6–4.8)	>43
Mouse	1.1 (1.2–1.5)	0.10 (0.082–0.12)	4.5 (3.1–6.9)
Rat	0.82 (0.63–1.1)	0.082 (0.069–0.099)	1.6 (1.2–2.0)
Dog	11 (8.8–12)	0.56 (0.48–0.65)	25 (21–29)
Rabbit	>41	ND	>43
Pig	>41	ND	ND
Monkey	>41	ND	ND

have conserved binding sites with human DHODH. DHODHs from the human malaria parasites, *P. falciparum* and *P. vivax*, and the simian parasite, *Plasmodium cynomolgi*, were inhibited by DSM265 with similar potency (Table 1). The IC_{50} for *Pv*DHODH was twofold higher than that for *Pf* DHODH, whereas for *P. cynomolgi*, it was twofold lower. In contrast, DSM265 had poor activity against DHODH from rodent *Plasmodium* species (*P. berghei* or *P. yoelii*) (*14*), and thus, efficacy models using these species have not been useful for profiling DSM265.

DSM430 and DSM450 also inhibit *Pf* DHODH, but their activity against *P. falciparum* parasites and their species selectivity profiles are substantially different (Table 1). The metabolite DSM450 was threefold less potent than DSM265 as a *Pf* DHODH inhibitor; however, it was 43-fold less active against *P. falciparum* 3D7 parasites [effective concentration (EC_{50}) = 0.079 μg/ml for DSM450 versus 0.0018 μg/ml for DSM265 (Fig. 2B)]; thus, it is not expected to contribute to in vivo parasite killing. The potency of the impurity of DSM430 was comparable to that of DSM265 against *Pf* DHODH, but it was 10-fold more potent on the tested mammalian enzymes (Table 1). DSM430 parasite activity exceeded that of DSM265 (Fig. 2B) (*P. falciparum* 3D7 EC_{50} = 0.0002 μg/ml). Given the lack of species selectivity of DSM430, concentrations of this impurity will need to be carefully controlled in clinical batches of DSM265. The reduced selectivity of DSM430 relative to the mammalian enzymes mirrors that of analogs containing *para* CF_3-aniline when combined with meta-fluorines (*16*).

Antimalarial activities of DSM265: Life cycle profiling and kill rate

DSM265 activity was profiled against the full range of parasite life cycle stages using strategies recently optimized with standard antimalarial compounds (*17*). In vitro blood-stage activity was evaluated for nine strains of *P. falciparum*, including chloroquine- and pyrimethamine-resistant parasites. DSM265 was equally effective (EC_{50} ranging from 0.001 to 0.004 μg/ml) against all tested strains (table S2). Notably, these EC_{50} values are lower than previous values determined in media containing 10% human serum (*14*), which is a reflection of differential DSM265 protein binding in different media (Table 2). The effects of DSM265 treatment (48 hours) on blood-stage parasites were evaluated by microscopy in comparison to standard antimalarial agents (Fig. 2C). DSM265 arrested parasites in the young trophozoite stage showing a profile similar to atovaquone. In contrast, pyrimethamine-treated parasites arrested as mature trophozoites and artemisinin-treated parasites were pyknotic.

In vitro DSM265 kill rates were determined for *P. falciparum* 3D7 parasites over a concentration range of 1 × EC_{50} (0.0046 μg/ml) to 100 × EC_{50} (Fig. 2, D and E, and fig. S3). DSM265 displayed maximum antimalarial effects at 3 × EC_{50} and above, requiring a 24- to 48-hour lag phase before parasite killing. At 1 × EC_{50}, DSM265 parasite killing was further delayed (96-hour lag phase) (fig. S3). Thus, 3 × EC_{50} (0.014 μg/ml; Table 2) represents the minimum concentration required to achieve the maximum kill rate (MPC) in vitro. The DSM265 kill rate was similar to atovaquone, but significantly slower than observed for artemisinin and chloroquine.

DSM265 liver-stage activity was evaluated in vitro against *P. falciparum* and *P. cynomolgi* liver-stage parasites. In the *P. falciparum* liver-stage assay, DSM265 was unable to block liver cell invasion, and small exoerythrocytic forms (EEFs) were observed after treatment except at the highest dose (4.2 μg/ml); the EEF count was reduced by treatment with primaquine (Fig. 3, A and B). However, DSM265 blocked EEF growth to the schizont stage with an EC_{50} of 0.0057 μg/ml (assessed by the diameter of the EEF), a value 30-fold more potent than that obtained for primaquine (EC_{50} primaquine = 0.15 μg/ml) (Fig. 3, C to E, and Table 2). The unbound EC_{50} for *P. falciparum* liver-stage large forms was similar to the unbound *P. falciparum* blood-stage EC_{50} (Table 2), suggesting that DSM265 will be effective for the elimination of both blood and liver replicative forms. In the *P. cynomolgi* liver-stage model, DSM265 was also active against the liver-stage large form (multinucleated schizont) (EC_{50} = 0.13 μg/ml), whereas it had poor activity against small forms representative of the nondividing hypnozoite, a surrogate for the dormant forms in *P. vivax* infections (fig. S4).

Activity of DSM265 on *P. falciparum* sexual and mosquito stages was also evaluated. It had no activity on early- or late-stage gametocytes and was inactive in the *P. falciparum* dual gamete formation assay (Table 2). DSM265 inhibited formation of multinucleated oocysts with an approximate unbound EC_{50} (38% inhibition) that was within threefold of the unbound EC_{50} against that of the blood-stage (Table 2). At the infection intensity observed in this study (22 oocysts per mosquito), reduced oocyst density did not translate into decreased numbers of infected mosquitoes. However, oocyst density in the field is much lower (one to three oocysts per mosquito), raising the possibility that there could be some transmission-blocking activity under these conditions.

In vivo parasite killing activity: Pharmacokinetic/pharmacodynamic relationships

To define the MPC required for parasite killing in vivo, we undertook a detailed analysis of the oral dose-response profile in the *P. falciparum* SCID mouse 4-day dosing model. Because the half-life of DSM265 in mice is much shorter (2 to 4 hours) than the predicted human half-life (described below), we dosed DSM265 twice daily to better mimic the sustained plasma exposure expected in humans. DSM265 had potent in vivo antimalarial activity with 90% effective dose (ED_{90}) of 3 mg/kg per day (1.5 mg/kg twice daily) (Fig. 4, table S3, and fig. S5), comparing favorably with chloroquine and mefloquine (table S3B). The maximum rate of parasite killing occurred at and above a dose of 13 mg/kg per day (6.4 mg/kg

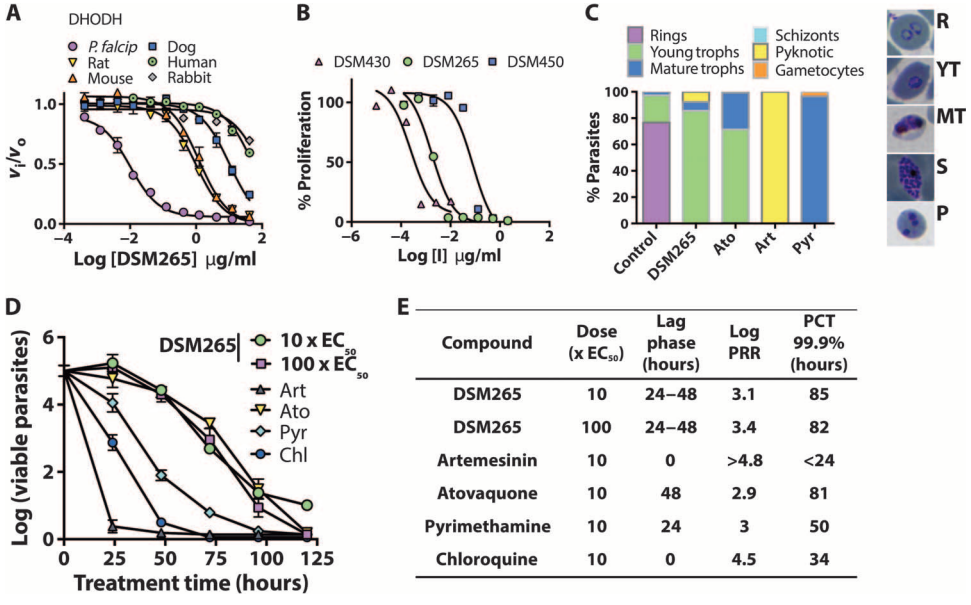

E

Compound	Dose (x EC_{50})	Lag phase (hours)	Log PRR	PCT 99.9% (hours)
DSM265	10	24–48	3.1	85
DSM265	100	24–48	3.4	82
Artemesinin	10	0	>4.8	<24
Atovaquone	10	48	2.9	81
Pyrimethamine	10	24	3	50
Chloroquine	10	0	4.5	34

Fig. 2. In vitro activity of DSM265 and its analogs on DHODH and *P. falciparum* parasites. (**A**) DHODH inhibition. IC_{50} values are reported in Table 1. Error bars show SEM for three technical replicates per concentration. Each fitted IC_{50} was obtained from 30 to 33 data points per fit. (**B**) In vitro *P. falciparum* 3D7 growth inhibition. Fitted EC_{50}s were 0.0018 μg/ml (0.0011 to 0.0028), 0.079 μg/ml (0.042 to 0.15), and 0.00020 μg/ml (0.00011 to 0.00056) for DSM265, DSM450, and DSM430, respectively, with the 95% confidence intervals in parenthesis (three technical replicates per concentration and 18 to 24 data points per fit; the plot shows mean ± SEM). (**C**) Effects on *P. falciparum* 3D7 blood-stage phenotype and development. Cells were treated with drug at 10 × EC_{50}, and parasites were evaluated by microscopy 48 hours after drug addition (minimally 200 cells were counted per condition). Atovaquone (Ato), artemisinin (Art), and pyrimethamine (Pyr) were used as controls. Images of representative parasites from the counted stages are displayed (R, rings; YT, young trophozoite; MT, mature trophozoite; S, schizont; P, pyknotic). (**D**) In vitro killing curves for treatment of *P. falciparum* 3D7 blood-stage parasites. Data for 10 × EC_{50} and 100 × EC_{50} (where EC_{50} = 0.0046 μg/ml) (four technical replicates showing the mean and SD) are displayed for DSM265. Data for artemisinin, atovaquone, pyrimethamine, and chloroquine (Chl) were previously reported (*33*). (**E**) Comparative DSM265 kill rates calculated from (D). PRR (parasite reduction ratio), the log number of parasites killed per asexual life cycle (48 hours); Lag phase, time before parasite killing begins; PCT (parasite clearance time), time to achieve 99.9% parasite kill. Primary data are provided in table S19.

twice daily) (Fig. 4A). Consistent with in vitro data (Fig. 2), a relatively steep dose-response relationship was observed in vivo. The maximum blood concentrations (C_{max}) and area under the blood concentration versus time profiles [day 1 area under the curve $(AUC)_{0–10\ h}$] were approximately dose proportional (Fig. 4B and table S3A). The DSM265 blood concentration at 23 hours after the last dose of 13 mg/kg per day (0.53 μg/ml, table S3A) was used as an estimate of the MPC, which corresponds to an unbound plasma concentration of 0.0011 μg/ml. This value shows good agreement with the unbound in vitro MPC (0.002 μg/ml) (Table 2). The ED_{90} in this SCID mouse study was 2.6-fold lower than that in a preliminary study in SCID mice dosed once daily, which was limited by a small-dose range and insufficient pharmacokinetic data to define the MPC (*14*).

Propensity of *P. falciparum* parasites to become resistant to DSM265

P. falciparum Dd2 and K1 parasites are multidrug-resistant strains commonly used to evaluate the propensity of parasites to become resistant to drugs in vitro (*18*). Dd2 parasites were selected under continuous DSM265 pressure at 3 × EC_{50} over a range of parasite inocula to evaluate the minimum inoculum for resistance (MIR), the lowest number of parasites necessary to generate a resistant mutant, using atovaquone as a comparator. The MIR for DSM265 averaged 2×10^6 (ranged 2×10^5 to 2×10^7) (table S4, A to C) over two independent

Table 2. DSM265 activity against *P. falciparum* parasites at different stages in the life cycle. Data represent EC_{50} values unless otherwise stated to be the minimum parasiticidal concentration (MPC).

Assay	MPC or EC_{50} (μg/ml)	Fraction unbound in assay media	Unbound MPC or EC_{50} (μg/ml)
Blood-stage: *P. falciparum* 3D7 in vitro MPC (kill assay)	0.014*	0.17†	0.0020
SCID mouse in vivo MPC (plasma)	1.1‡	0.001§	0.0011
Blood-stage: *P. falciparum* 3D7 in vitro growth assay	0.0046*	0.17†	0.00078
Liver-stage: *P. falciparum* to schizont	0.0057	0.215¶	0.0012
P. falciparum early-stage gametocytes stages III to IV; strain NF54	>0.42	0.004‖	>0.0017
Gametocyte assay *P. falciparum* stages IV to V	Inactive >16	ND	ND
P. falciparum dual gamete formation assay	Inactive >42	ND	ND
P. falciparum stage V oocyst	38% at 1.0	0.001§	38% at 0.001

*Data taken from Fig. 2D. †AlbuMAX II (0.5%) in RPMI 1640. ‡Blood to plasma ratio in the humanized SCID mouse of 0.5 was used to convert blood concentrations to plasma concentrations. §Human plasma. ¶Fetal calf serum (10%) in Dulbecco's modified Eagle's medium or similar medium. ‖Human serum (10%) in RPMI 1640.

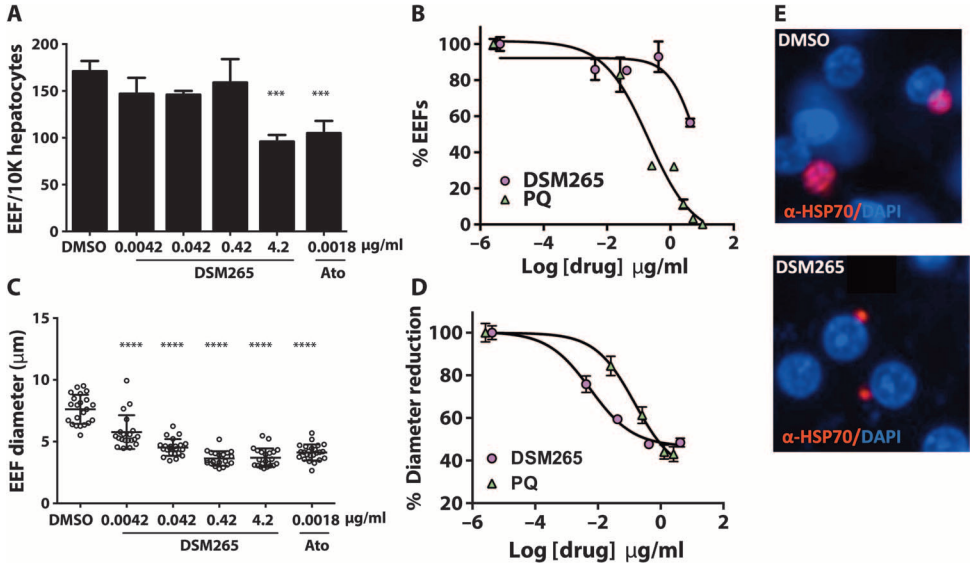

Fig. 3. Activity of DSM265 against *P. falciparum* liver stages. (**A**) Inhibitory effect on hepatocyte infection rate. Number of EEF/10,000 hepatocytes quantitated at different concentrations of DSM265 relative to the dimethyl sulfoxide (DMSO) control for three technical replicates using the same human donor; error bars show the SD for the replicates. Primary data are provided in table S20. (**B**) Dose-response curve showing the effect of DSM265 and primaquine (PQ) on infection rate. Primaquine EC_{50} = 0.20 μg/ml (0.059 to 0.71) and DSM265 EC_{50} = 7.0 μg/ml (4.3 to 11) (n = 3). Errors are SEM. (**C**) Inhibitory effect on EEF diameter for n = 20 to 22 EEFs. (**D**) Dose-response curve showing the effect on EEF size. Primaquine EC_{50} = 0.15 μg/ml (0.11 to 0.20) and for DSM265 EC_{50} = 0.0057 (0.0048 to 0.0069) μg/ml. Error bars show the SD for n = 20 to 22. (**E**) Representative images of parasites day 3 after infection treated with DMSO or DSM265 (0.42 μg/ml). Statistical significance was determined by analysis of variance [ANOVA; ***P = 0.0002, ****P < 0.0001; for comparison of drug-treated to DMSO controls (A and C)]. Historical data for primaquine (B and D) and atovaquone (A and C) using the same donor are shown. HSP70, heat shock protein 70; DAPI, 4′,6-diamidino-2-phenylindole.

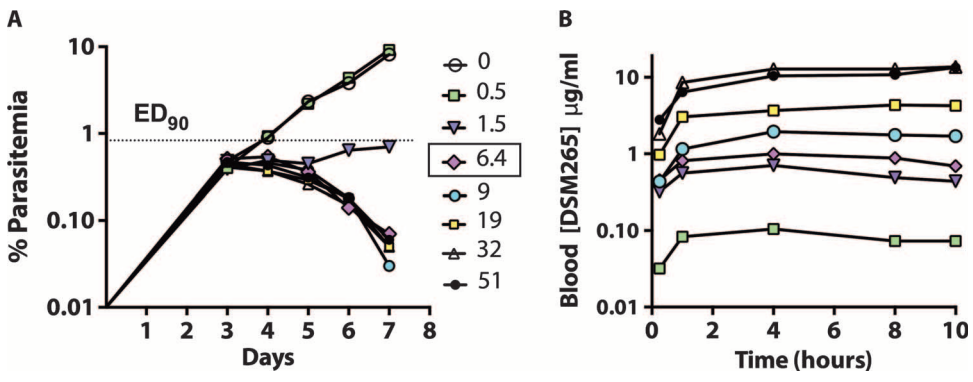

Fig. 4. In vivo efficacy of DSM265 in the *P.falciparum*–infected SCID mouse. DSM265 was dosed as the tosylate salt twice daily for 4 days starting on day 3 after infection. (**A**) Blood parasitemia versus days after infection for administered doses (mg/kg per 12 hours). The ED_{90} (1.5 mg/kg per 12 hours) and the MPC (dose = 6.4 mg/kg per 12 hours) were determined 24 hours after the last dose. The parasite detection limit was 0.01%. (**B**) DSM265 blood concentrations (μg/ml) over 10 hours after the first dose for doses as indicated. A single data point was collected per dose with the exception of the no-drug control where n = 3 biological replicates were obtained. Primary data are provided in table S3 (C and D).

studies, whereas for atovaquone, the MIR was 2×10^7 (table S4, B and D). The EC_{50} for DSM265-resistant Dd2 parasites increased 3- to 26-fold (Table 3 and table S5) over wild-type parasites compared to a 10-fold shift observed for atovaquone (table S4D). The effect of DSM265 concentrations on propensity for resistance was also studied: drug concentrations of 33 × EC_{50} were required to suppress emergence of atovaquone-resistant parasites compared to only 8 × EC_{50} for DSM265 for a similar inoculum (2×10^7 parasites) (table S4, A and B). Additional selections at higher DSM265 concentrations (5 × EC_{50} to 8 × EC_{50}) were also performed at a high starting inoculum (2×10^9) (table S4C). Clonal lines from these selections showed EC_{50} shifts of ~30-fold (table S5). Selection of DSM265-resistant parasites was significantly more difficult with the K1 strain (MIR of 2×10^8) (table S4E). Resistant parasites were not obtained from selections with the HB3 strain at any DSM265 concentration, whereas resistant HB3 parasites could be obtained for selections with atovaquone (table S4F). DSM265-resistant isolates derived from Dd2 and K1 remained fully sensitive to atovaquone and artemisinin (table S5).

The resistance mechanism was evaluated for clonal Dd2 lines selected at 3 × EC_{50}. Both amplification of the DHODH gene and acquisition of a point mutation (G181C) were observed (Table 3 and table S5), consistent with DHODH being the primary target of parasite killing. The G181C mutation maps to the DSM265 binding site where this residue makes close contacts with the $-CF_2CH_3$ group (Fig. 1). Introduction of the G181C mutation into recombinant *Pf* DHODH showed that the IC_{50} was 13-fold higher than that for the wild-type enzyme, which correlates with the 26-fold shift in parasite EC_{50}. Steady-state kinetic analysis of G181C *Pf* DHODH showed that k_{cat} was reduced by twofold compared to wild-type, whereas the K_m for CoQ_d and L-DHO was unchanged (table S6).

Drug synergy studies to identify possible combination partners

To determine whether DSM265 has synergistic or antagonistic activity with possible partner compounds, interactions between DSM265 and other reported antimalarials were evaluated using the fixed-ratio isobologram method (table S7). Compounds tested included several artemisinin derivatives, the synthetic ozonide OZ439, chloroquine, piperaquine, pyronaridine, mefloquine, lumefantrine, atovaquone, proguanil, and the dihydrofolate reductase inhibitors P218 and pyrimethamine. DSM265 activity was additive with all tested compounds, and no evidence of synergistic or antagonistic activity was found.

Table 3. Evaluation of in vitro generated DSM265 Dd2–resistant parasites. Fold change in parentheses. *Pf*DHODH data are IC_{50} values determined on the recombinant wild-type (wt) or G181C mutant *P. falciparum* enzymes. All data were collected with a minimum of three technical replicates and then used for a global fit. Error analysis is provided in table S5. N/A, not applicable.

Clone number	Inoculum	DSM265 selection concentration (μg/ml)	DSM265 Dd2 EC_{50} (μg/ml)	Gene copy number	DHODH mutation	*Pf*DHODH IC_{50} (μg/ml)
Dd2/wt	N/A	N/A	0.0022	1.0	N/A	0.0096
PR.Cl1	2×10^7	0.0083	0.0083 (3.8)	2.7	None	N/A
PR.Cl2	2×10^7	0.0083	0.0099 (4.5)	2.3	None	N/A
DF.R10 Clb	2×10^6	0.0095	0.058 (26)	1.1	G181C	0.120 (12)

Physicochemical properties, in vitro ADME, and metabolite identification

Progression of DSM265 toward clinical development required detailed studies to define properties related to absorption, distribution, metabolism, and excretion (ADME). DSM265 free base was shown to be chemically stable in the solid state after storage at 30°C/65% relative humidity for up to 24 months, but degradation of both the DSM265 free base and tosylate salt was observed when solutions were subjected to simulated sunlight necessitating that solutions be protected from light (table S8A). DSM265 free base had poor aqueous solubility under simulated gastric conditions (6.8 μg/ml) and in fasted- and fed-state simulated intestinal fluids (5.1 and 27.6 μg/ml, respectively) (table S8B). Across Caco-2 cell monolayers, DSM265 had high apical to basolateral permeability ($P_{app} > 30 \times 10^{-6}$ cm/s), with minimal evidence of efflux, suggesting that it is likely to be well absorbed in vivo. The P-glycoprotein and breast cancer resistance protein inhibitors verapamil and fumitremorgin C, respectively, had no effect on DSM265 permeability, indicating that it is not a substrate for these transporters. High permeability integrated with low aqueous solubility suggested that DSM265 is a biopharmaceutics classification system (BCS) class II compound.

Plasma protein binding of DSM265 was highest in human plasma (99.9%), with slightly lower values in mouse and dog plasma (99.7 and 99.4%, respectively), and the lowest binding in rat plasma (97.7%) (table S9). Because of the high plasma protein binding, DSM265 had a blood to plasma partitioning ratio of 0.5 to 0.7 across species (table S9).

In hepatic microsomes and cryopreserved hepatocytes, DSM265 exhibited minimal degradation across species, consistent with low in vivo hepatic clearance (table S9). In vitro studies with individual human cytochrome P450 (CYP) enzymes (Supersomes) indicated a low extent of metabolism in the presence of CYP2C8 (0.032 μl/min per pmol CYP) and CYP2C19 (0.039 μl/min per pmol CYP), whereas no measurable loss was observed with the other tested CYP isoforms (table S9).

DSM265 metabolite identification and profiling was conducted using pooled plasma samples obtained from single-dose pharmacokinetic studies in animals. Five metabolites were identified (tables S10 and S11 and fig. S6) with metabolism primarily occurring via monooxidation to form the circulating metabolite M4 [DSM450 identity confirmed by chemical synthesis (Fig. 1)], followed by glucuronidation to give M2 and M3, and dehydration to form M5. On the basis of mass spectrometry peak area ratios, M4 (DSM450) was estimated to be the main plasma metabolite in all species, representing 4 to 27% of the parent AUC with other metabolites being minor.

In vivo pharmacokinetic properties and formulation studies

To support toxicological studies and human dose predictions and to test formulation performance, a series of pharmacokinetic studies were conducted in rodents, dogs, and monkeys. Consistent with previous data in rodents (*14*), the DSM265 pharmacokinetic profile in monkeys and dogs after intravenous dosing was characterized by very low plasma clearance, moderate to high volume of distribution, and a long half-life (10 to 45 hours) (table S12). Oral pharmacokinetic studies in dogs suggested that increases in AUC were dose proportional at lower doses (3 and 30 mg/kg) but less so at higher doses (tables S13 and S14). The oral bioavailability of DSM265 was moderate in dogs (~20%); however, there was evidence of enterohepatic recirculation, with secondary peaks noted after feeding (Fig. 5). Increases in C_{max} and AUC were observed when DSM265 was administered orally to dogs with food (Fig. 5 and table S14).

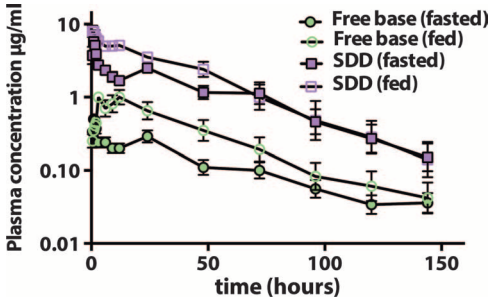

Fig. 5. Oral pharmacokinetic profiles for DSM265 in dogs. Pharmacokinetic behavior of DSM265 was evaluated after a single oral dose (10 mg/kg) of either free base as a suspension in 0.5% carboxymethyl cellulose, 0.4% Tween 80, or SDD formulation administered as a suspension in Methocel A4M, in either the fasted or the fed state. Data represent mean ± SEM for six dogs. Primary data are provided in table S21.

Salt selection studies identified the tosylate salt based on improved solubility in water (threefold). It showed improved exposure in mice, but not in rats and dogs (tables S13 and S14). Efforts to increase the dissolution and absorption profile of crystalline DSM265 free base included particle size reduction (nanomilling) and preparation of amorphous spray dried dispersions (SDD; containing 25% DSM265 load), with the latter increasing solubility in simulated intestinal fluids to about 100 μg/ml. After oral dosing to dogs, increases in C_{max} and AUC were obtained with the nanomilled free base or with the free base SDD formulation (Fig. 5 and table S14). The SDD formulation all but eliminated the food effect in dogs (table S14) and was selected for further development. The amorphous properties of the SDD formulation were stable for at least up to 9 months at 40°C/75% relative humidity.

Human pharmacokinetic predictions

Human pharmacokinetic parameters were estimated using a physiologically based pharmacokinetic (PBPK) model inputting experimental values for physicochemical properties, permeability, protein binding, and erythrocyte partitioning. Because the in vitro intrinsic clearance determined in liver

microsomes and hepatocytes underestimated the observed in vivo clearance in all species tested, allometric scaling of the unbound in vivo clearance in preclinical species was used to estimate a human clearance value of 0.25 liter/hour. The PBPK model predicted a human volume of distribution of 46 liters and a half-life of about 130 hours. Human plasma concentration versus time profiles were simulated for different dose levels (fig. S7) and suggested that a single dose in the range of 200 to 400 mg would likely maintain plasma concentrations above the plasma MPC (1 to 2 μg/ml) for at least 8 days.

In vitro safety assessment

Safety of DSM265 was assessed in a series of standard in vitro assays (table S15). DSM265 showed minimal activity in a standard panel of 106 human receptors and ion channels (IC_{50} > 4.2 μg/ml for the full panel) performed by Cerep Inc. and when tested against a panel of human kinases (University of Dundee). In human liver microsomes in vitro, DSM265 caused no measurable inhibition of any of the key CYP enzymes (IC_{50} >10 μg/ml) (table S15) and did not induce CYP enzymes in human hepatocytes (table S15).

Genotoxicity

DSM265 and SF_5-aniline (synthetic precursor) were tested in a conventional five-strain bacterial reverse mutation assay (Ames test) for mutagenic activity (table S15). There was no increase in the number of revertant colonies for either compound, and both were judged to be nonmutagenic. Genotoxicity was also studied in an oral bone marrow micronucleus test in male CD1 mice (table S15). There was no increase in micronucleated polychromatic erythrocytes in this study; thus, combined with the negative result in the Ames test, it was concluded that DSM265 was not genotoxic.

Evaluation of cardiac electrophysiological risk

DSM265 was tested for activity against the human ether-a-go-go–related gene (hERG) K^+ channel in a standard patch clamp assay. Inhibition of this channel has been associated with QT prolongation and arrhythmias (*19*). DSM265 showed some inhibition of the hERG channel (IC_{50} = 0.66 to 2.9 μg/ml; table S15). Notably, the predicted unbound maximum plasma concentration (C_{max} < 0.01 μg/ml) of DSM265 in humans (fig. S7) is 70- to 320-fold lower than the IC_{50} for hERG channel inhibition, suggesting a very low likelihood of an interaction with the channel in humans at the expected therapeutic dose. To further assess its potential cardiac risk, DSM265 was tested in a rabbit cardiac ventricular wedge assay; no torsade de pointes (TdP)–type arrhythmias were observed (tested up to 5 μg/ml). DSM265 did not cause any significant prolongation of the QT and Tp-e interval at 1 or 0.5 Hz, and there was no change in the ratio of Tp-e/QT interval (fig. S8). Tp-e duration and the ratio of Tp-e/QT interval reflect dispersion of repolarization, and increases in these parameters are thought to elevate the risk of TdP arrhythmia (*19*, *20*). As a final confirmation, cardiac safety was evaluated by telemetry in vivo in conscious dogs at DSM265 oral doses of 30 and 300 mg/kg (plasma concentrations 24 hours after the high dose were 1.3 μg/ml) (table S16). All electrocardiographs (ECGs) were within normal limits, and there were no other adverse effects on cardiac rate, rhythm, or blood pressure.

Exploratory toxicology studies

Safety of DSM265 was evaluated in rats, mice, and dogs in both single-dose and repeat-dose oral toxicity studies (table S16). In the repeat-dose studies, mice and rats were dosed daily; however, dogs were dosed every other day as the long half-life was expected to lead to significant accumulation. Dogs were dosed in the fed state to increase exposure. In the 7-day repeat-dose study in rats, the maximum tolerated dose (MTD) was 50 mg/kg per day for both males and females. Rats showed weight loss, signs of dehydration (for example, increased blood urea nitrogen and hematocrit), decreases in white blood cell counts, and gastrointestinal tract damage that was dose-dependent. As this was an early-stage exploratory study, toxicokinetic data were not collected. We reasoned that the significant sensitivity of rat DHODH to DSM265 (IC_{50} = 0.82 μg/ml) combined with the lower plasma protein binding and higher unbound concentrations relative to other species (table S9) resulted in the rat being atypically sensitive to DSM265, making it a poor model to study potential DSM265 toxicity in humans. It was therefore decided to evaluate the toxicological effects of DSM265 in mice and dogs, as both species had plasma protein binding levels that were similar to humans, and dog DHODH was significantly less sensitive to DSM265 inhibition than the rat enzyme.

DSM265 was well tolerated at all dose levels in mice (25 to 200 mg/kg per day once daily for 7 days) and dogs (30 to 480 mg/kg every other day for 10 days), and there were no mortalities in either species. In mice, there was no observation of clinical effects or noted changes in pathology. In dogs receiving the highest dose, there were instances of vomiting and reduced food consumption. A slight increase in bilirubin was also observed, but this was not accompanied by changes in any other liver function markers. On the basis of these data, the MTD in both species was considered to have exceeded the highest dose (MTD >200 mg/kg in mice and MTD >480 mg/kg in dogs). Toxicokinetic analysis confirmed that plasma exposure in both species increased with increasing dose (tables S17 and S18). There was no evidence of DSM265 accumulation over the 7-day study in mice, but despite the alternate day dose regimen in dogs, significant accumulation was still apparent.

The average plasma concentration within a dosing interval (C_{av}) has been suggested to be a useful parameter for evaluation of safety margins in toxicology studies (*21*). Plasma C_{av} values at the highest dose tested in the mouse (C_{av} = 11.7 μg/ml, day 7) and dog (C_{av} = 16.4 μg/ml, day 1) were 10- and 15-fold higher, respectively, than the MPC for maximum parasite clearance in the SCID mouse efficacy study (Table 2). Full toxicokinetic data were not collected in the dog after the final dose so C_{av} could not be calculated, but given the noted accumulation, the margin in dogs is likely to be about twofold higher than that calculated from day 1 data.

Evaluation of safety in G6PD-deficient mice

Because of the prevalence of G6PD-deficient patients in malaria endemic regions (*1*), DSM265 was tested for evidence of hemolytic toxicity in nonobese diabetic (NOD)–SCID mice engrafted with blood type A G6PD-deficient human RBCs. DSM265 was not hemolytic in this model, suggesting that it will be safe for dosing in G6PD-deficient patients (fig. S9). In contrast, treatment with primaquine led to a substantial loss in human RBCs and an increase in mouse reticulocytes and resulted in a substantial increase in spleen weight.

DISCUSSION

The triazolopyrimidine-based inhibitor DSM265 represents a new class of antimalarial agent and is the first compound targeting plasmodial DHODH to reach clinical development. DSM265 fits a unique niche in the worldwide antimalarial portfolio, displaying both blood- and liver-stage activity, and a sufficiently long predicted human half-life to support either single-dose treatment or once-weekly dosing for chemoprevention, giving it considerable advantage over current agents that are dosed daily or lack liver-stage

activity. Herein, we have described a comprehensive set of assays profiling biological activity, pharmacokinetic properties, and safety, all of which support the advancement of DSM265 to clinical trials to evaluate safety and efficacy in humans.

The activities of DSM265 across the *Plasmodium* life cycle are consistent with its mechanism of action in blocking formation of nucleotides required for RNA and DNA synthesis. DSM265 inhibited formation of blood- and liver-stage parasites with similar potency, arresting growth before formation of the multinucleated schizont stage in both cases. Modest activity against formation of the multinucleated insect stage (oocyst) was also observed, suggesting that DSM265 could exert some transmission-blocking activity, particularly if dosed with a gametocytocidal agent. DSM265 blocked growth earlier in the parasite life cycle than did pyrimethamine, likely because of the fact that DSM265 acts upstream of dihydrofolate reductase inhibitors in the pyrimidine biosynthetic pathway. The earlier growth arrest of DSM265-treated parasites may be a consequence of RNA depletion, because growth arrest appears to precede the burst of DNA biosynthesis required for schizont formation.

DHODH is a long-duration compound with a predicted human half-life of more than 100 hours and with the potential to be useful for either treatment or prevention of malaria. Minimal metabolism by hepatic CYP enzymes and very high plasma protein binding both likely contribute to the sustained exposure after oral dosing. For *P. falciparum*, a single dose of 200 to 400 mg is predicted to maintain plasma concentrations above the MPC for at least 8 days. DSM265 is one of only a handful of compounds with potent activity on liver-stage parasites, distinguishing it from many other compounds in the malaria drug portfolio (*9*, *17*). Indeed, of the phase 2 clinical candidates, the only other agent with liver-stage activity is KAF156 (*22*), and it has an observed human half-life that is shorter than that predicted for DSM265 (*23*). Recently, a new preclinical candidate targeting *P. falciparum* translation elongation factor was reported to have blood- and liver-stage activity as well as transmission-blocking activity, but this compound, although promising, is still in early-stage preclinical development (*24*) and, unlike DSM265, has not yet advanced to human clinical trials. Although compounds lacking liver-stage activity have been used for chemoprevention (for example, chloroquine and mefloquine), liver-stage activity would be expected to boost prophylactic potential, particularly for compounds like DSM265 that show a lag phase before blood-stage killing begins. Although DSM265 blocks formation of the liver-stage schizont, it apparently lacks activity against hypnozoites (based on the *P. cynomolgi* data). Thus, DSM265 would not be useful for radical cure of *P. vivax*. DSM265's activity profile is most similar to atovaquone and other cytochrome bc_1 inhibitors (for example, ELQ-300) (*25*), which also block uridine nucleotide biosynthesis. However, notably, a long-duration compound such as DSM265 has potential advantages for use in chemoprevention compared to atovaquone, which is dosed daily.

Careful monitoring for development of resistance against clinically used antimalarials is clearly of paramount importance given the history of drugs lost due to widespread resistance. The multidrug-resistant *P. falciparum* Dd2 strain developed resistance to DSM265 relatively easily, with a profile similar to atovaquone at low drug concentrations. However, at higher concentrations, or in other strains, it was significantly more difficult to select for DSM265-resistant parasites, suggesting that overall, it may be harder for resistance to DSM265 to emerge compared to atovaquone. Published data on chloroquine and KAF156 suggest a lower propensity to develop resistance than DSM265 (MIR of 10^8 in Dd2 using the same $3 \times EC_{50}$ protocol) (*22*, *26*). Similar data are not available for the ATP4 inhibitor (KAE609) in clinical development, although its target was identified through sequencing of resistant parasites (*27*). However, an MIR as low as 10^7 against *P. falciparum* 3D7 was recently reported for another ATP4 inhibitor (SJ733) (*28*). It is not known how these in vitro data will translate to the clinical situation, but clearly, our findings point to the need to closely monitor for the emergence of DSM265-resistant parasites during clinical development.

Mechanistic studies indicated that DSM265 resistance was linked to increased DHODH gene copy number or to point mutations in the inhibitor binding pocket, providing easy markers to monitor resistance in the field. Both mechanisms appear to be common routes for the parasite to develop resistance after in vitro selection with DHODH inhibitors. Selection with a related triazolopyrimidine DSM1 also led to gene amplification (*29*), whereas point mutations in the inhibitor binding site were observed after selection using several unrelated chemical series in addition to another triazolopyrimidine DSM74, although the G181C mutation that we observed in parasites resistant to DSM265 was not identified in that study (*30*). If resistant parasites emerge readily in early clinical studies, DSM265, like atovaquone, might be best positioned for chemoprevention. Long-duration compounds with potential for preventative treatment are particularly needed in areas of seasonal malaria transmission (*1*), and DSM265 appears particularly well suited to this application. Given the historical precedence for resistance, even for drugs lacking a specific protein target (for example, chloroquine), it is clear that a combination strategy is the only mechanism to prolong the usefulness of new clinical agents against malaria (*10*). DSM265 will be formulated in combination with another antimalarial compound to mitigate this risk. We found through drug combination tests that DSM265 antimalarial activity was additive with a wide selection of potential partner compounds; thus, these compounds remain viable partners for DSM265.

DSM265 showed excellent safety in short-term multiple-dose studies in mice and dogs, but it was less well tolerated in rats. Significant species differences were identified both in the inhibitory activity of DSM265 toward DHODH from various mammalian species and in plasma protein binding. These data suggested that higher unbound concentrations coupled with significant DHODH inhibition led to greater toxicity in rats. This hypothesis is supported by the observation that only in rats were the toxicological findings suggestive of a direct effect on the myeloid elements of the bone marrow, similar to those reported for the immunosuppressive drug leflunomide, a clinically used DHODH inhibitor (*31*, *32*). As human DHODH is much less sensitive to DSM265 inhibition than are the rodent and dog enzymes, similar toxicological effects are not expected to occur in humans. Although there was evidence of low micromolar activity against the hERG channel in vitro, the unbound concentration in vivo will likely be too low for an interaction with the channel to occur. Cardiovascular studies in dogs showed no evidence of any effect on the ECG or any evidence that DSM265 has the potential to cause cardiac arrhythmias.

The discovery and development of DSM265 is a rare example of a target-based strategy leading to identification of a new antimalarial, because most compounds in the pipeline have been identified by phenotypic screens (*5*). The advantage of the target-based approach is that it provided a clear path to development both by simplifying lead optimization and by allowing us to understand the toxicological findings in the rat and to move beyond them. Thus, knowledge of the target has been essential to the successful advancement of DSM265. The preclinical development studies described herein, combined with a favorable toxicity profile, led to selection of DSM265 as a clinical development candidate and to advancement into phase 1 human studies. Although the studies described herein are expected to be very predictive of a desirable outcome in humans, they are limited by their restriction to in vitro analysis and the use of animal

models. The full potential of DSM265 as a drug to treat malaria will not be fully defined until data from human safety and efficacy studies are collected and reported. In particular, whether the human half-life and dose prediction accurately reflect what is observed in humans, whether the predicted efficacy is observed against the range of *Plasmodium* species present in the field, and to what extent drug resistance is observed when the compound is used to treat human patients are open questions. Finally, the choice of whether DSM265 should be advanced for treatment or chemoprevention will depend on both progress made with other compounds in the pipeline and on the ongoing safety and efficacy evaluation of DSM265 in humans.

MATERIALS AND METHODS

Study design

The program objectives were to characterize the efficacy, pharmacokinetic properties, and safety of DSM265 to support its preclinical development and to enable the compound to advance to human clinical trials. Efficacy was evaluated at both the enzyme target level and against the parasite using in vitro and in vivo models of *Plasmodium* infection. Enzyme inhibitor activity was evaluated against a range of different *Plasmodium* and mammalian species to demonstrate activity and to show selectivity relative to both human and other mammalian species that would be used in toxicological models. Studies of *Plasmodium* growth or infection were designed to evaluate efficacy across the full range of life cycle stages, to determine how fast the compound kills parasites, to obtain preliminary data on possible drug resistance mechanisms based on in vitro selection, and to define the pharmacokinetic/pharmacodynamic relationship. Drug-like properties were evaluated using a series of in vitro ADME studies, and pharmacokinetic analysis was performed across multiple species. Finally both in vitro and in vivo toxicological profiling was undertaken to assess safety.

Animal welfare

Animal experiments were approved by the institutional animal care and use committees for each of the experimental sites. All studies were conducted according to the appropriate legislation and institutional policies on the care and use of animals.

DSM265 synthesis, impurities, and metabolite synthesis

Synthesis of DSM265. DSM265 (2-(1,1-difluoroethyl)-5-methyl-[*N*-[4-(pentafluorosulfanyl)phenyl]1,2,4]triazolo[1,5-*a*]pyrimidin-7-amine) was prepared as previously described (*14*) to good manufacturing practice (GMP) standards at 14-kg scale (99.2% purity) by WuXi AppTec (scheme S1). The major impurity (about 0.6%) in this batch was DSM430 (Fig. 1), which derives from an impurity in the SF_5-aniline raw material.

Synthesis of DSM430. DSM430 (2-(1,1-difluoroethyl)-*N*-(3-fluoro-4-(pentafluoro-L^6-sulfanyl)phenyl)-5-methyl-[1,2,4]triazolo[1,5-*a*]pyrimidin-7-amine) was synthesized using the same basic scheme as for DSM265 (scheme S1) to 99% purity. Experimental data are as follows: MS 430.1; nuclear magnetic resonance (NMR; D6-DMSO) shows peaks at 2.15 (3H, t), 2.51 (3H, s), 6.95 (1H, s), 7.5 to 7.6 (2H, m), and 8.05 (1H, m). ^{19}F NMR ($CDCl_3$) shows peaks at −104 ppm (parts per million) (aromatic F), −90.5 ppm (CF_3), and −68.8 ppm (SF_5).

Synthesis of DSM450. DSM450 (2-(1,1-difluoroethyl)-7-((4-(pentafluoro-L^6-sulfanyl)phenyl)amino)-[1,2,4]triazolo[1,5-*a*]pyrimidin-5-yl)methanol) was identified as the major in vivo metabolite of DSM265 and was synthesized to 99% purity by Syngene (scheme S2). Experimental data are as follows: mass/charge ratio (*m*/*z*) 432.0 (M^+) ^1H NMR (400 MHz, DMSO-d6): δ 10.79 (s, 1H), 8.03 (d, J = 8.8 Hz, 2H), 7.69 (d, J = 8.6 Hz, 2H), 6.90 (s, 1H), 5.70 (t, J = 5.84 Hz, 3H), 4.53 (d, J = 5.92 Hz, 2H), 2.13 (t, 19.1 Hz 3H).

Nomenclature

We use the nomenclature EC_{50} for concentration-response curves on parasites, whereas we use IC_{50} for enzyme data because this distinction helps clarify whether the data are cell- or enzyme-based.

DHODH purification and assays

DHODHs were expressed as recombinant proteins in *Escherichia coli* and purified as previously described (*14*, *16*). New expression constructs are described in Supplementary Materials and Methods. Steady-state kinetic analysis was performed using a 2,5-dichloroindophenol–based spectrophotometric method as described (*14*). Enzyme and substrate concentrations were DHODH 5 to 10 nM and L-dihydroorotate 0.2 mM and CoQd 0.02 mM. DSM265 stock solutions (100×) were made in DMSO. Data were fitted to the log[I] versus response (three parameters) equation or for compounds where the IC_{50} >10 μM to the standard IC_{50} equation [$Y = 1/(1 + X/(IC_{50}))$] in GraphPad Prism. Error represents the 95% confidence interval of the fit.

X-ray structure determination

The x-ray structure of *Pf* DHODH in complex with DSM265 was solved as described in Supplementary Materials and Methods. The structure was displayed with PyMOL (PyMOL Molecular Graphics System, DeLano Scientific, San Carlos, CA, 2000).

In vitro parasite efficacy assays

Blood-stage assays. *P. falciparum* cells were propagated in RPMI 1640 containing 0.5% AlbuMAX II (*14*). EC_{50} determinations for *P. falciparum* 3D7 cells and drug-resistant parasites were performed using the SYBR Green 72-hour growth assay (*16*). Phenotypic assessment of blood-stage 3D7 parasites before and after treatment of DSM265 in comparison to control compounds was conducted at 10× IC_{50}. Initial parasitemia was 1% (92% rings) at a hematocrit of 2%. Parasites were stained with Giemsa after drug exposure (48 hours) and scored by microscopy with minimally 200 cells per condition. Parasite kill curves were assessed on *P. falciparum* 3D7 cells by incubating parasites with drug for the indicated time followed by washing and replating in drug-free media to assess the number of remaining viable parasites as described (*33*). EC_{50} values reported for this study are for a 48-hour growth assay.

Liver-stage assays. *P. falciparum* NF54 liver-stage assays were performed in media containing 10% fetal calf serum as described (*34*). Statistical significance was determined by ordinary one-way ANOVA with Dunnett's multiple comparison using GraphPad Prism.

Sexual-stage assays. Assays were performed as described in Supplementary Materials and Methods.

Curve fitting. For EC_{50} determinations, data were fitted to the log(inhibitor) versus response – variable slope (four-parameter) model in GraphPad Prism, and error represents the 95% confidence interval of the fit.

Selection of DSM265-resistant parasites in vitro

Asynchronous cultures of cloned *P. falciparum* Dd2, K1, and HB3 parasite lines grown in culture medium containing 0.5% AlbuMAX were used in continuous challenge experiments (*29*, *35*). Cultures were maintained under DSM265 selection pressure for a minimum of 60 days. Gene copy number was determined as described (*29*).

In vivo parasite efficacy assays

SCID mouse efficacy study. NOD-*scid IL-2Rγ*^{null} (NSG) mice (Jackson Laboratory) (23 to 36 g) engrafted with human erythrocytes (*36*) were infected with 20×10^6 *P. falciparum* Pf3D7$_{0087/N9}$ by intravenous injection. DSM265 tosylate salt or chloroquine was administered orally in vehicle [saline solution for chloroquine; 0.5% (w/v) sodium carboxymethyl cellulose, 0.5% (v/v) benzyl alcohol, 0.4% (v/v) Tween 80 in water for DSM265]. DSM265 was administered twice daily at target doses ranging from 0.5 to 75 mg/kg (free base equivalent) starting on day 3 after infection. Formulation concentrations were measured to obtain actual doses administered. Parasitemia was monitored by flow cytometry. Blood DSM265 levels were measured by liquid chromatography–tandem mass spectrometry (LC-MS/MS) as described (*14*). Human biological samples were sourced ethically, and their research use was in accordance with the terms of the informed consents.

Pharmacokinetic studies, physiochemical, and in vitro ADME studies

Pharmacokinetic studies were conducted in female Swiss outbred mice, male Sprague-Dawley rats, male beagle dogs, and female macaque monkeys. DSM265 was administered intravenously and orally in a range of formulations. Blood samples were collected into tubes containing anticoagulant, plasma was separated by centrifugation, and DSM265 and metabolite concentrations were determined by LC-MS. Physiochemical and in vitro ADME study methods are described in Supplementary Materials and Methods.

Prediction of human pharmacokinetic parameters and human dose

Human clearance was estimated by allometric scaling of the unbound in vivo clearance in mice, rats, dogs, and monkeys. Distributional processes were estimated using a PBPK model (GastroPlus, Simulations Plus Inc.), inputting the estimated human clearance, the measured log $D_{pH\ 7.4}$, apparent solubility from the amorphous SDD formulation, Caco-2 permeability, plasma protein binding, and blood to plasma ratio. Human plasma concentration versus time profiles were simulated for different dose levels to estimate the dose range that would provide concentrations above the MPC (1 to 2 μg/ml) for a period of more than 8 days.

CYP inhibition and induction

CYP inhibition studies were performed using a substrate-specific approach in human liver microsomes. Methods for this assay and for CYP induction assays are described in Supplementary Materials and Methods.

Rabbit wedge

The rabbit ventricular wedge assay was performed as described (*20*) (Supplementary Materials and Methods).

Hemolytic toxicity assay

Testing for hemolytic toxicity in G6PD-deficient human RBCs was performed in NOD-SCID mice engrafted with blood from a G6PD A– donor (*37*).

Genotoxicity

Ames testing. DSM265 and the SF_5-aniline (synthetic precursor) were examined for mutagenic activity in the *Salmonella typhimurium–E. coli*/microsome plate incorporation assay (Supplementary Materials and Methods).

In vivo genotoxicity study. The in vivo micronuclei study was performed in male CD-1 mice under good laboratory practice (GLP) conditions (Supplementary Materials and Methods).

Toxicology studies in rats, mice, and dogs

Exploratory and GLP toxicological studies were performed in rats, mice, and dogs (full details provided in Supplementary Materials and Methods). Animals were monitored daily for clinical changes. Body weight and food consumption were also monitored. Hematology, clinical chemistry, and histopathology were performed by standard methods. Dog cardiac studies were performed by standard methods.

Statistical analysis

Statistical analyses were performed using GraphPad Prism 6.0 (GraphPad Inc.). Ordinary one-way ANOVA with Dunnett's multiple comparison or one-way ANOVA with Bonferroni's posttest was used to compare three or more groups. For enzyme and parasite IC_{50} or EC_{50} determination, data were fitted to the specified model as described in Materials and Methods using nonlinear least squares analysis, and the mean and 95% confidence intervals are reported. Minimally, triplicate data were collected for each compound concentration, and error bars on graphs represent the SEM. Pharmacokinetic data were collected typically for two to six animals, and SD is provided for data sets containing $n > 2$. Details specific to each study are provided in the figure legends.

SUPPLEMENTARY MATERIALS

www.sciencetranslationalmedicine.org/cgi/content/full/7/296/296ra111/DC1
Synthesis
Materials and Methods
Fig. S1. (Fo-Fc) map for DSM265:*Pf*DHODH binding site.
Fig. S2. DHODH sequence alignment.
Fig. S3. In vitro parasite killing curves.
Fig. S4. Activity of DSM265 against *P. cynomolgi* large (liver schizonts) and small (hypnozoite) forms.
Fig. S5. The effect of DSM265 treatment on *P. falciparum Pf*3D70087/N9 in vivo.
Fig. S6A. Proposed biotransformation pathways of DSM265 in plasma of mice, rabbits, monkeys, and dogs.
Fig. S6B. Plasma concentrations of DSM265 and DSM450 (hydroxy metabolite).
Fig. S7. Simulated human plasma profiles using a PBPK model (GastroPlus).
Fig. S8. Effect on ECG in the rabbit cardiac ventricular wedge assay.
Fig. S9. Evaluation of the effects of DSM265 on G6PD-deficient human RBCs engrafted into a NOD-SCID mouse.
Table S1. *Pf*DHODH-DSM265 x-ray diffraction data and refinement statistics.
Table S2. In vitro antimalarial activity of DSM265.
Table S3A. Blood pharmacokinetic data for DSM265 in SCID mice.
Table S3B. SCID mouse in vivo antimalarial activity.
Table S3C. SCID mouse parasitemia.
Table S3D. SCID mouse pharmacokinetic individual time point data.
Table S4A. Selection for DSM265-resistant parasites in *P. falciparum* Dd2: Rathod laboratory.
Table S4B. Selection for atovaquone-resistant parasites in *P. falciparum* Dd2: Rathod laboratory.
Table S4C. Selection for DSM265-resistant parasites in *P. falciparum* Dd2: Fidock laboratory.
Table S4D. Selection for atovaquone-resistant parasites in *P. falciparum* Dd2: Fidock laboratory.
Table S4E. Selection for DSM265-resistant parasites in *P. falciparum* K1: Fidock laboratory.
Table S4F. Selection for DSM265 and atovaquone *P. falciparum* HB3: Rathod laboratory.
Table S5. Summary of DSM265-resistant clones: Analysis of parasites in whole-cell assays.
Table S6. Kinetic analysis of *Pf*DHODH mutants.
Table S7. Drug combination analysis.
Table S8A. Stability data for DSM265 free base and tosylate salt.
Table S8B. Solubility data for DSM265 free base.
Table S9. In vitro ADME data for DSM265.
Table S10. In vivo metabolite identification.
Table S11. Relative plasma exposures of DSM265 metabolites in mice, rabbits, monkeys, and dogs.
Table S12. DSM265 plasma pharmacokinetics after a single intravenous dose in mice, rats, dogs, and monkey.
Table S13. DSM265 plasma pharmacokinetics after a single oral dose of DSM265 in mice, rats,

dogs, and monkeys.
Table S14. Effect of salt form, formulation, and food on the DSM265 plasma pharmacokinetics after oral dosing in beagle dogs.
Table S15. Safety pharmacology.
Table S16. Exploratory toxicology studies (non-GLP) in rodents and dogs.
Table S17A. Toxicokinetic parameters on days 1 and 7 in a mouse 7-day toxicology study.
Table S17B. Individual mouse plasma concentrations 7-day toxicology study 25 mg/kg.
Table S17C. Individual mouse plasma concentrations 7-day toxicology study 75 mg/kg.
Table S17D. Individual mouse plasma concentrations 7-day toxicology study 200 mg/kg.
Table S18A. Toxicokinetic data from a 10-day toxicology study in male beagle dogs.
Table S18B. Toxicokinetic parameters day 1 of toxicology study in male beagle dogs.
Table. S19. Primary data supporting Fig. 2.
Table. S20. Primary data supporting Fig. 3 (A and B).
Table. S21. Primary data supporting Fig. 5.
References (*38*–*66*)

REFERENCES AND NOTES

1. N. J. White, S. Pukrittayakamee, T. T. Hien, M. A. Faiz, O. A. Mokuolu, A. M. Dondorp, Malaria. *Lancet* **383**, 723–735 (2014).
2. L. H. Miller, H. C. Ackerman, X. Z. Su, T. E. Wellems, Malaria biology and disease pathogenesis: Insights for new treatments. *Nat. Med.* **19**, 156–167 (2013).
3. World Malaria Report (World Health Organization, Geneva, 2014); www.who.int/malaria/publications/world_malaria_report_2014/en.
4. C. Cotter, H. J. Sturrock, M. S. Hsiang, J. Liu, A. A. Phillips, J. Hwang, C. S. Gueye, N. Fullman, R. D. Gosling, R. G. Feachem, The changing epidemiology of malaria elimination: New strategies for new challenges. *Lancet* **382**, 900–911 (2013).
5. J. N. Burrows, E. Burlot, B. Campo, S. Cherbuin, S. Jeanneret, D. Leroy, T. Spangenberg, D. Waterson, T. N. Wells, P. Willis, Antimalarial drug discovery—The path towards eradication. *Parasitology* **141**, 128–139 (2014).
6. R. N. Price, F. Nosten, Single-dose radical cure of *Plasmodium vivax*: A step closer. *Lancet* **383**, 1020–1021 (2014).
7. D. Menard, F. Ariey, Towards real-time monitoring of artemisinin resistance. *Lancet Infect. Dis.* **15**, 367–368 (2015).
8. M. P. Anthony, J. N. Burrows, S. Duparc, J. J. Moehrle, T. N. Wells, The global pipeline of new medicines for the control and elimination of malaria. *Malar. J.* **11**, 316 (2012).
9. Y. Yuthavong, B. Tarnchompoo, T. Vilaivan, P. Chitnumsub, S. Kamchonwongpaisan, S. A. Charman, D. N. McLennan, K. L. White, L. Vivas, E. Bongard, C. Thongphanchang, S. Taweechai, J. Vanichtanankul, R. Rattanajak, U. Arwon, P. Fantauzzi, J. Yuvaniyama, W. N. Charman, D. Matthews, Malarial dihydrofolate reductase as a paradigm for drug development against a resistance-compromised target. *Proc. Natl. Acad. Sci. U.S.A.* **109**, 16823–16828 (2012).
10. S. Duparc, C. Lanza, D. Ubben, I. Borghini-Fuhrer, L. Kellam, Optimal dose finding for novel antimalarial combination therapy. *Trop. Med. Int. Health* **17**, 409–413 (2012).
11. J. N. Burrows, R. H. van Huijsduijnen, J. J. Möhrle, C. Oeuvray, T. N. Wells, Designing the next generation of medicines for malaria control and eradication. *Malar. J.* **12**, 187 (2013).
12. P. A. Stocks, V. Barton, T. Antoine, G. A. Biagini, S. A. Ward, P. M. O'Neill, Novel inhibitors of the *Plasmodium falciparum* electron transport chain. *Parasitology* **141**, 50–65 (2014).
13. M. A. Phillips, P. K. Rathod, Plasmodium dihydroorotate dehydrogenase: A promising target for novel anti-malarial chemotherapy. *Infect. Disord. Drug Targets* **10**, 226–239 (2010).
14. J. M. Coteron, M. Marco, J. Esquivias, X. Deng, K. L. White, J. White, M. Koltun, F. El Mazouni, S. Kokkonda, K. Katneni, R. Bhamidipati, D. M. Shackleford, I. Angulo-Barturen, S. B. Ferrer, M. B. Jiménéz-Díaz, F. J. Gamo, E. J. Goldsmith, W. N. Charman, I. Bathurst, D. Floyd, D. Matthews, J. N. Burrows, P. K. Rathod, S. A. Charman, M. A. Phillips, Structure-guided lead optimization of triazolopyrimidine-ring substituents identifies potent *Plasmodium falciparum* dihydroorotate dehydrogenase inhibitors with clinical candidate potential. *J. Med. Chem.* **54**, 5540–5561 (2011).
15. R. Gujjar, F. El Mazouni, K. L. White, J. White, S. Creason, D. M. Shackleford, X. Deng, W. N. Charman, I. Bathurst, J. Burrows, D. M. Floyd, D. Matthews, F. S. Buckner, S. A. Charman, M. A. Phillips, P. K. Rathod, Lead optimization of aryl and aralkyl amine based triazolopyrimidine inhibitors of *Plasmodium falciparum* dihydroorotate dehydrogenase with anti-malarial activity in mice. *J. Med. Chem.* **54**, 3935–3949 (2011).
16. X. Deng, S. Kokkonda, F. El Mazouni, J. White, J. N. Burrows, W. Kaminsky, S. A. Charman, D. Matthews, P. K. Rathod, M. A. Phillips, Fluorine modulates species selectivity in the triazolopyrimidine class of *Plasmodium falciparum* dihydroorotate dehydrogenase inhibitors. *J. Med. Chem.* **57**, 5381–5394 (2014).
17. M. Delves, D. Plouffe, C. Scheurer, S. Meister, S. Wittlin, E. A. Winzeler, R. E. Sinden, D. Leroy, The activities of current antimalarial drugs on the life cycle stages of *Plasmodium*: A comparative study with human and rodent parasites. *PLOS Med.* **9**, e1001169 (2012).
18. X. C. Ding, D. Ubben, T. N. Wells, A framework for assessing the risk of resistance for anti-malarials in development. *Malar. J.* **11**, 292 (2012).
19. P. J. Kannankeril, D. M. Roden, When should QT be measured? Summer solstice or Christmas Eve? *Heart Rhythm* **4**, 282–283 (2007).
20. T. Liu, B. S. Brown, Y. Wu, C. Antzelevitch, P. R. Kowey, G. X. Yan, Blinded validation of the isolated arterially perfused rabbit ventricular wedge in preclinical assessment of drug-induced proarrhythmias. *Heart Rhythm* **3**, 948–956 (2006).
21. D. A. Smith, P. Morgan, W. M. Vogel, D. K. Walker, The use of C_{av} rather than AUC in safety assessment. *Regul. Toxicol. Pharmacol.* **57**, 70–73 (2010).
22. K. L. Kuhen, A. K. Chatterjee, M. Rottmann, K. Gagaring, R. Borboa, J. Buenviaje, Z. Chen, C. Francek, T. Wu, A. Nagle, S. W. Barnes, D. Plouffe, M. C. Lee, D. A. Fidock, W. Graumans, M. van de Vegte-Bolmer, G. J. van Gemert, G. Wirjanata, B. Sebayang, J. Marfurt, B. Russell, R. Suwanarusk, R. N. Price, F. Nosten, A. Tungtaeng, M. Gettayacamin, J. Sattabongkot, J. Taylor, J. R. Walker, D. Tully, K. P. Patra, E. L. Flannery, J. M. Vinetz, L. Renia, R. W. Sauerwein, E. A. Winzeler, R. J. Glynne, T. T. Diagana, KAF156 is an antimalarial clinical candidate with potential for use in prophylaxis, treatment, and prevention of disease transmission. *Antimicrob. Agents Chemother.* **58**, 5060–5067 (2014).
23. F. J. Leong, R. Zhao, S. Zeng, B. Magnusson, T. T. Diagana, P. Pertel, A first-in-human randomized, double-blind, placebo-controlled, single- and multiple-ascending oral dose study of novel imidazolopiperazine KAF156 to assess its safety, tolerability, and pharmacokinetics in healthy adult volunteers. *Antimicrob. Agents Chemother.* **58**, 6437–6443 (2014).
24. B. Baragaña, I. Hallyburton, M. C. Lee, N. R. Norcross, R. Grimaldi, T. D. Otto, W. R. Proto, A. M. Blagborough, S. Meister, G. Wirjanata, A. Ruecker, L. M. Upton, T. S. Abraham, M. J. Almeida, A. Pradhan, A. Porzelle, M. S. Martínez, J. M. Bolscher, A. Woodland, S. Norval, F. Zuccotto, J. Thomas, F. Simeons, L. Stojanovski, M. Osuna-Cabello, P. M. Brock, T. S. Churcher, K. A. Sala, S. E. Zakutansky, M. B. Jiménez-Díaz, L. M. Sanz, J. Riley, R. Basak, M. Campbell, V. M. Avery, R. W. Sauerwein, K. J. Dechering, R. Noviyanti, B. Campo, J. A. Frearson, I. Angulo-Barturen, S. Ferrer-Bazaga, F. J. Gamo, P. G. Wyatt, D. Leroy, P. Siegl, M. J. Delves, D. E. Kyle, S. Wittlin, J. Marfurt, R. N. Price, R. E. Sinden, E. A. Winzeler, S. A. Charman, L. Bebrevska, D. W. Gray, S. Campbell, A. H. Fairlamb, P. A. Willis, J. C. Rayner, D. A. Fidock, K. D. Read, I. H. Gilbert, A novel multiple-stage antimalarial agent that inhibits protein synthesis. *Nature* **522**, 315–320 (2015).
25. A. Nilsen, A. N. LaCrue, K. L. White, I. P. Forquer, R. M. Cross, J. Marfurt, M. W. Mather, M. J. Delves, D. M. Shackleford, F. E. Saenz, J. M. Morrisey, J. Steuten, T. Mutka, Y. Li, G. Wirjanata, E. Ryan, S. Duffy, J. X. Kelly, B. F. Sebayang, A. M. Zeeman, R. Noviyanti, R. E. Sinden, C. H. Kocken, R. N. Price, V. M. Avery, I. Angulo-Barturen, M. B. Jiménez-Díaz, S. Ferrer, E. Herreros, L. M. Sanz, F. J. Gamo, I. Bathurst, J. N. Burrows, P. Siegl, R. K. Guy, R. W. Winter, A. B. Vaidya, S. A. Charman, D. E. Kyle, R. Manetsch, M. K. Riscoe, Quinolone-3-diarylethers: A new class of antimalarial drug. *Sci. Transl. Med.* **5**, 177ra137 (2013).
26. R. A. Cooper, M. T. Ferdig, X. Z. Su, L. M. Ursos, J. Mu, T. Nomura, H. Fujioka, D. A. Fidock, P. D. Roepe, T. E. Wellems, Alternative mutations at position 76 of the vacuolar transmembrane protein PfCRT are associated with chloroquine resistance and unique stereospecific quinine and quinidine responses in *Plasmodium falciparum*. *Mol. Pharmacol.* **61**, 35–42 (2002).
27. N. J. White, S. Pukrittayakamee, A. P. Phyo, R. Rueangweerayut, F. Nosten, P. Jittamala, A. Jeeyapant, J. P. Jain, G. Lefèvre, R. Li, B. Magnusson, T. T. Diagana, F. J. Leong, Spiroindolone KAE609 for falciparum and vivax malaria. *N. Engl. J. Med.* **371**, 403–410 (2014).
28. M. B. Jiménez-Díaz, D. Ebert, Y. Salinas, A. Pradhan, A. M. Lehane, M. E. Myrand-Lapierre, K. G. O'Loughlin, D. M. Shackleford, M. Justino de Almeida, A. K. Carrillo, J. A. Clark, A. S. Dennis, J. Diep, X. Deng, S. Duffy, A. N. Endsley, G. Fedewa, W. A. Guiguemde, M. G. Gómez, G. Holbrook, J. Horst, C. C. Kim, J. Liu, M. C. Lee, A. Matheny, M. S. Martínez, G. Miller, A. Rodríguez-Alejandre, L. Sanz, M. Sigal, N. J. Spillman, P. D. Stein, Z. Wang, F. Zhu, D. Waterson, S. Knapp, A. Shelat, V. M. Avery, D. A. Fidock, F. J. Gamo, S. A. Charman, J. C. Mirsalis, H. Ma, S. Ferrer, K. Kirk, I. Angulo-Barturen, D. E. Kyle, J. L. DeRisi, D. M. Floyd, R. K. Guy, (+)-SJ733, a clinical candidate for malaria that acts through ATP4 to induce rapid host-mediated clearance of *Plasmodium*. *Proc. Natl. Acad. Sci. U.S.A.* **111**, E5455–E5462 (2014).
29. J. L. Guler, D. L. Freeman, V. Ahyong, R. Patrapuvich, J. White, R. Gujjar, M. A. Phillips, J. DeRisi, P. K. Rathod, Asexual populations of the human malaria parasite, *Plasmodium falciparum*, use a two-step genomic strategy to acquire accurate, beneficial DNA amplifications. *PLOS Pathog.* **9**, e1003375 (2013).
30. L. S. Ross, F. J. Gamo, M. J. Lafuente-Monasterio, O. M. Singh, P. Rowland, R. C. Wiegand, D. F. Wirth, In vitro resistance selections for *Plasmodium falciparum* dihydroorotate dehydrogenase inhibitors give mutants with multiple point mutations in the drug-binding site and altered growth. *J. Biol. Chem.* **289**, 17980–17995 (2014).
31. H. I. Keen, P. G. Conaghan, S. E. Tett, Safety evaluation of leflunomide in rheumatoid arthritis. *Expert Opin. Drug Saf.* **12**, 581–588 (2013).
32. Leflunomide FDA Drug Approval Package: NDA 20905 (U.S. Food and Drug Administration, Baltimore, MD, 1998); www.accessdata.fda.gov/drugsatfda_docs/nda/98/20905_arava.cfm.
33. L. M. Sanz, B. Crespo, C. De-Cózar, X. C. Ding, J. L. Llergo, J. N. Burrows, J. F. Garciá-Bustos, F. J. Gamo, *P. falciparum* in vitro killing rates allow to discriminate between different antimalarial mode-of-action. *PLOS One* **7**, e30949 (2012).
34. S. March, S. Ng, S. Velmurugan, A. Galstian, J. Shan, D. J. Logan, A. E. Carpenter, D. Thomas, B. K. Sim, M. M. Mota, S. L. Hoffman, S. N. Bhatia, A microscale human liver platform that supports the hepatic stages of *Plasmodium falciparum* and *vivax*. *Cell Host Microbe* **14**, 104–115 (2013).
35. E. H. Ekland, J. Schneider, D. A. Fidock, Identifying apicoplast-targeting antimalarials using high-throughput compatible approaches. *FASEB J.* **25**, 3583–3593 (2011).
36. M. B. Jiménez-Díaz, T. Mulet, S. Viera, V. Gómez, H. Garuti, J. Ibáñez, A. Alvarez-Doval, L. D. Shultz, A. Martínez, D. Gargallo-Viola, I. Angulo-Barturen, Improved murine model of malaria using

Plasmodium falciparum competent strains and non-myelodepleted NOD-*scid IL2Rγ*^{null} mice engrafted with human erythrocytes. *Antimicrob. Agents Chemother.* **53**, 4533–4536 (2009).
37. R. Rochford, C. Ohrt, P. C. Baresel, B. Campo, A. Sampath, A. J. Magill, B. L. Tekwani, L. A. Walker, Humanized mouse model of glucose 6-phosphate dehydrogenase deficiency for in vivo assessment of hemolytic toxicity. *Proc. Natl. Acad. Sci. U.S.A.* **110**, 17486–17491 (2013).
38. J. Baldwin, C. H. Michnoff, N. A. Malmquist, J. White, M. G. Roth, P. K. Rathod, M. A. Phillips, High-throughput screening for potent and selective inhibitors of *Plasmodium falciparum* dihydroorotate dehydrogenase. *J. Biol. Chem.* **280**, 21847–21853 (2005).
39. N. A. Malmquist, R. Gujjar, P. K. Rathod, M. A. Phillips, Analysis of flavin oxidation and electron-transfer inhibition in *Plasmodium falciparum* dihydroorotate dehydrogenase. *Biochemistry* **47**, 2466–2475 (2008).
40. M. A. Phillips, R. Gujjar, N. A. Malmquist, J. White, F. El Mazouni, J. Baldwin, P. K. Rathod, Triazolopyrimidine-based dihydroorotate dehydrogenase inhibitors with potent and selective activity against the malaria parasite, *Plasmodium falciparum*. *J. Med. Chem.* **51**, 3649–3653 (2008).
41. X. Deng, R. Gujjar, F. El Mazouni, W. Kaminsky, N. A. Malmquist, E. J. Goldsmith, P. K. Rathod, M. A. Phillips, Structural plasticity of malaria dihydroorotate dehydrogenase allows selective binding of diverse chemical scaffolds. *J. Biol. Chem.* **284**, 26999–27009 (2009).
42. Z. Otwinowski, W. Minor, C. W. Carter Jr., Processing of X-ray diffraction data collected in oscillation mode. *Methods Enzymol.* **276**, 307–326 (1997).
43. P. R. Evans, An introduction to data reduction: Space-group determination, scaling and intensity statistics. *Acta Crystallogr. D Biol. Crystallogr.* **67**, 282–292 (2011).
44. A. J. McCoy, Solving structures of protein complexes by molecular replacement with Phaser. *Acta Crystallogr. D Biol. Crystallogr.* **63**, 32–41 (2007).
45. P. D. Adams, P. V. Afonine, G. Bunkóczi, V. B. Chen, I. W. Davis, N. Echols, J. J. Headd, L. W. Hung, G. J. Kapral, R. W. Grosse-Kunstleve, A. J. McCoy, N. W. Moriarty, R. Oeffner, R. J. Read, D. C. Richardson, J. S. Richardson, T. C. Terwilliger, P. H. Zwart, *PHENIX*: A comprehensive Python-based system for macromolecular structure solution. *Acta Crystallogr. D Biol. Crystallogr.* **66**, 213–221 (2010).
46. P. Emsley, B. Lohkamp, W. G. Scott, K. Cowtan, Features and development of *Coot*. *Acta Crystallogr. D Biol. Crystallogr.* **66**, 486–501 (2010).
47. L. Dembele, A. Gego, A. M. Zeeman, J. F. Franetich, O. Silvie, A. Rametti, R. Le Grand, N. Dereuddre-Bosquet, R. Sauerwein, G. J. van Gemert, J. C. Vaillant, A. W. Thomas, G. Snounou, C. H. Kocken, D. Mazier, Towards an in vitro model of *Plasmodium* hypnozoites suitable for drug discovery. *PLOS One* **6**, e18162 (2011).
48. A. M. Zeeman, S. M. van Amsterdam, C. W. McNamara, A. Voorberg-van der Wel, E. J. Klooster, A. van den Berg, E. J. Remarque, D. M. Plouffe, G. J. van Gemert, A. Luty, R. Sauerwein, K. Gagaring, R. Borboa, Z. Chen, K. Kuhen, R. J. Glynne, A. K. Chatterjee, A. Nagle, J. Roland, E. A. Winzeler, D. Leroy, B. Campo, T. T. Diagana, B. K. Yeung, A. W. Thomas, C. H. Kocken, KAI407, a potent non-8-aminoquinoline compound that kills *Plasmodium cynomolgi* early dormant liver stage parasites in vitro. *Antimicrob. Agents Chemother.* **58**, 1586–1595 (2014).
49. S. D'Alessandro, F. Silvestrini, K. Dechering, Y. Corbett, S. Parapini, M. Timmerman, L. Galastri, N. Basilico, R. Sauerwein, P. Alano, D. Taramelli, A *Plasmodium falciparum* screening assay for anti-gametocyte drugs based on parasite lactate dehydrogenase detection. *J. Antimicrob. Chemother.* **68**, 2048–2058 (2013).
50. S. Duffy, V. M. Avery, Identification of inhibitors of *Plasmodium falciparum* gametocyte development. *Malar. J.* **12**, 408 (2013).
51. M. J. Delves, C. Ramakrishnan, A. M. Blagborough, D. Leroy, T. N. Wells, R. E. Sinden, A high-throughput assay for the identification of malarial transmission-blocking drugs and vaccines. *Int. J. Parasitol.* **42**, 999–1006 (2012).
52. M. J. Delves, A. Ruecker, U. Straschil, J. Lelièvre, S. Marques, M. J. López-Barragán, E. Herreros, R. E. Sinden, Male and female *Plasmodium falciparum* mature gametocytes show different responses to antimalarial drugs. *Antimicrob. Agents Chemother.* **57**, 3268–3274 (2013).
53. C. Snyder, J. Chollet, J. Santo-Tomas, C. Scheurer, S. Wittlin, In vitro and in vivo interaction of synthetic peroxide RBx11160 (OZ277) with piperaquine in *Plasmodium* models. *Exp. Parasitol.* **115**, 296–300 (2007).
54. Q. L. Fivelman, I. S. Adagu, D. C. Warhurst, Modified fixed-ratio isobologram method for studying in vitro interactions between atovaquone and proguanil or dihydroartemisinin against drug-resistant strains of *Plasmodium falciparum*. *Antimicrob. Agents Chemother.* **48**, 4097–4102 (2004).
55. S. Schleiferböck, C. Scheurer, M. Ihara, I. Itoh, I. Bathurst, J. N. Burrows, P. Fantauzzi, J. Lotharius, S. A. Charman, J. Morizzi, D. M. Shackleford, K. L. White, R. Brun, S. Wittlin, In vitro and in vivo characterization of the antimalarial lead compound SSJ-183 in *Plasmodium* models. *Drug Des. Devel. Ther.* **7**, 1377–1384 (2013).
56. E. Jantratid, N. Janssen, C. Reppas, J. B. Dressman, Dissolution media simulating conditions in the proximal human gastrointestinal tract: An update. *Pharm. Res.* **25**, 1663–1676 (2008).
57. D. M. Roden, P. Kannankeril, D. Darbar, On the relationship among QT interval, atrial fibrillation, and torsade de pointes. *Europace* **9**, iv1–iv3 (2007).
58. H. R. Lu, E. Vlaminckx, A. Van de Water, J. Rohrbacher, A. Hermans, D. J. Gallacher, In-vitro experimental models for the risk assessment of antibiotic-induced QT prolongation. *Eur. J. Pharmacol.* **577**, 222–232 (2007).
59. K. Mortelmans, E. Zeiger, The Ames *Salmonella*/microsome mutagenicity assay. *Mutat. Res.* **455**, 29–60 (2000).
60. K. Mortelmans, E. S. Riccio, The bacterial tryptophan reverse mutation assay with *Escherichia coli* WP2. *Mutat. Res.* **455**, 61–69 (2000).
61. S. Deferme, R. Mols, W. Van Driessche, P. Augustijns, Apricot extract inhibits the P-gp–mediated efflux of talinolol. *J. Pharm. Sci.* **91**, 2539–2548 (2002).
62. Q. Mao, J. D. Unadkat, Role of the breast cancer resistance protein (ABCG2) in drug transport. *AAPS J.* **7**, E118–E133 (2005).
63. Y. H. Zhao, J. Le, M. H. Abraham, A. Hersey, P. J. Eddershaw, C. N. Luscombe, D. Butina, G. Beck, B. Sherborne, I. Cooper, J. A. Platts, Evaluation of human intestinal absorption data and subsequent derivation of a quantitative structure–activity relationship (QSAR) with the Abraham descriptors. *J. Pharm. Sci.* **90**, 749–784 (2001).
64. V. B. Chen, W. B. Arendall III, J. J. Headd, D. A. Keedy, R. M. Immormino, G. J. Kapral, L. W. Murray, J. S. Richardson, D. C. Richardson, *MolProbity*: All-atom structure validation for macromolecular crystallography. *Acta Crystallogr. D Biol. Crystallogr.* **66**, 12–21 (2010).
65. J. L. Vennerstrom, S. Arbe-Barnes, R. Brun, S. A. Charman, F. C. Chiu, J. Chollet, Y. Dong, A. Dorn, D. Hunziker, H. Matile, K. McIntosh, M. Padmanilayam, J. Santo Tomas, C. Scheurer, B. Scorneaux, Y. Tang, H. Urwyler, S. Wittlin, W. N. Charman, Identification of an antimalarial synthetic trioxolane drug development candidate. *Nature* **430**, 900–904 (2004).
66. R. L. Brent, The history of the editorship of Teratology during the period from July 1, 1976 to January 1, 1993. *Teratology* **63**, 100–105 (2001).

Acknowledgments: We thank L. D. Shultz and the Jackson Laboratory for providing access to NSG mice through their collaboration with GlaxoSmithKline Tres Cantos Medicines Development Campus. We are also indebted to T. Wells for thoroughly reviewing the manuscript. Results shown in this report are derived from work performed at Argonne National Laboratory, Structural Biology Center at the Advanced Photon Source. Argonne is operated by UChicago Argonne, LLC, for the U.S. Department of Energy, Office of Biological and Environmental Research under contract DE-AC02-06CH11357. **Funding:** This work was supported by funds from the U.S. NIH grants U01AI075594 (to I.B., M.A.P., P.K.R., and S.A.C.) and R01AI103947 (to M.A.P. and P.K.R.) and from Medicines for Malaria Venture (MMV). M.A.P. acknowledges the support of the Welch Foundation (I-1257). M.A.P. holds the Beatrice and Miguel Elias Distinguished Chair in Biomedical Science and the Carolyn R. Bacon Professorship in Medical Science and Education. Biomedical Primate Research Centre (BBRC) (A.M.-Z. and C.K.) and Columbia University (C.L.N. and D.A.F.) were supported by funding from the MMV. BBRC was also supported by a translational research grant (WT078285) from the Wellcome Trust. **Author contributions:** M.A.P. and S.A.C. wrote the paper and contributed to overall study design and data interpretation; M.A.P. and F.E.M. designed, performed, and/or analyzed studies on enzyme inhibition; X. Deng and D.R.T. performed the protein x-ray crystallography; S.A.C., K.L.W., K.M., and Y.L. designed, supervised, and/or analyzed ADME and pharmacokinetic studies; P.K.R., S.K., T.L., and J.N.B. performed or supervised chemical synthesis; J.W., J.W.N., P.K.R., M.A.P., C.L.N., and D.A.F. designed, performed, or analyzed studies on in vitro drug resistance; S.N.B., S.M., S.W., M.L.-M., F.J.G.B., L.M.S.A., M.S.M., M.B.J.-D., S.F.B., I.A.-B., A.M.-Z., C.K., R. Sauerwein, K.D., V.M.A., S.D., M.D., R. Sinden, A.R., I.B., X. Ding, B.C., D.L., J.N.B., and M.A.P. designed, performed, and/or analyzed in vitro and in vivo parasite efficacy studies; J.N.H., J. Louttit, Y.C., and A.S. performed, designed, or interpreted rabbit wedge studies; J. Lotharius, A.D., K.M., J.M., and T.R. designed and supervised toxicologic studies; J.G., L.I., E.R., K.S.W., and R.R. performed or supervised in vivo toxicologic studies in mice, rats, or dogs; and A.D., K.M., J.M., and M.J.R. interpreted the results from toxicologic studies. **Competing interests:** M.A.P., S.A.C., P.K.R., and J.N.B. hold a pending patent covering DSM265 and related compounds (antimalarial agents that are inhibitors of DHODH, WO2011/041304). T.L. and A.D. are paid consultants to MMV. S.B. is a paid consultant to Hepregen. R.S. and K.D. hold stock in TropIQ. **Data and materials availability:** The x-ray structures of DSM265 bound to *Pf*DHODH have been deposited in the PDB database [form I (4RX0) and form II (5BOO)], and the DNA sequence of mini-pig DHODH has been deposited to GenBank (KR108306).

Submitted 16 January 2015
Accepted 26 June 2015
Published 15 July 2015
10.1126/scitranslmed.aaa6645

Citation: M. A. Phillips, J. Lotharius, K. Marsh, J. White, A. Dayan, K. L. White, J. W. Njoroge, F. El Mazouni, Y. Lao, S. Kokkonda, D. R. Tomchick, X. Deng, T. Laird, S. N. Bhatia, S. March, C. L. Ng, D. A. Fidock, S. Wittlin, M. Lafuente-Monasterio, F. J. G. Benito, L. M. S. Alonso, M. S. Martinez, M. B. Jimenez-Diaz, S. F. Bazaga, I. Angulo-Barturen, J. N. Haselden, J. Louttit, Y. Cui, A. Sridhar, A.-M. Zeeman, C. Kocken, R. Sauerwein, K. Dechering, V. M. Avery, S. Duffy, M. Delves, R. Sinden, A. Ruecker, K. S. Wickham, R. Rochford, J. Gahagen, L. Iyer, E. Riccio, J. Mirsalis, I. Bathhurst, T. Rueckle, X. Ding, B. Campo, D. Leroy, M. J. Rogers, P. K. Rathod, J. N. Burrows, S. A. Charman, A long-duration dihydroorotate dehydrogenase inhibitor (DSM265) for prevention and treatment of malaria. *Sci. Transl. Med.* **7**, 296ra111 (2015).

Science Translational Medicine AAAS

A long-duration dihydroorotate dehydrogenase inhibitor (DSM265) for prevention and treatment of malaria

Margaret A. Phillips *et al.*

Sci Transl Med **7**, 296ra111 (2015);
DOI: 10.1126/scitranslmed.aaa6645

Editor's Summary

Long-acting new treatment for drug-resistant malaria

Malaria kills 0.6 million people annually, yet current malaria drugs are no longer fully effective because the parasite that causes malaria is becoming resistant to these agents. Phillips *et al.* have identified a new drug that kills both drug-sensitive and drug-resistant malaria parasites by targeting the ability of the parasite to synthesize the nucleotide precursors required for synthesis of DNA and RNA. This drug kills parasites in both the blood and liver and is sufficiently long-acting that it is expected to cure malaria after a single dose or to be effective if dosed weekly for chemoprevention.

Science Translational Medicine (print ISSN 1946-6234; online ISSN 1946-6242) is published weekly, except the last week in December, by the American Association for the Advancement of Science, 1200 New York Avenue NW, Washington, DC 20005.